Invited Articles

Lubricated-to-frictional shear thickening scenario in dense suspensions

Jeffrey F. Morris*

Benjamin Levich Institute and Department of Chemical Engineering, CUNY City College of New York, New York, New York 10031, USA

(Received 31 July 2018; published 21 November 2018)

Shear thickening is the increase of viscosity as shear rate or stress increases. For concentrated or dense suspensions of solid particles, this phenomenon may take the extreme form known as discontinuous shear thickening (DST). In DST, the relative viscosity η_r exhibits a discontinuous variation when presented as a function of the shear rate $\dot{\gamma}$, typically with a large jump in viscosity at the discontinuity; $\eta_r(\phi) = \eta(\phi)/\eta_0$, with η_0 the suspending fluid viscosity and ϕ the solid volume fraction. Rate dependence implies that η_r is a function not only of ϕ but also of $\dot{\gamma}$ or the shear stress σ. A scenario in which the close interactions between particles undergo a stress-driven lubricated-to-frictional (LF) transition provides a coherent mechanistic basis for the shear thickening seen in dense suspensions. Prior study of shear thickening leading to the proposal of the LF transition is briefly reviewed. The LF scenario and its predictions are presented, along with a perspective on unresolved issues on widely different scales, from contact interactions to system-spanning force networks.

DOI: 10.1103/PhysRevFluids.3.110508

I. INTRODUCTION

Shear thickening is defined by the condition that the viscosity of a flowing material increases with shear rate, i.e., $\partial\eta/\partial\dot{\gamma} > 0$, which may in some cases be more conveniently stated as $\partial\eta/\partial\sigma > 0$, with σ the shear stress. The present work provides a brief review of investigations of shear thickening in concentrated suspensions and a perspective arising from my own study directed toward establishing a coherent mechanism to rationalize the various forms of shear thickening seen in suspensions. For decades, shear thickening has been experimentally observed to occur in suspensions, as described in the following section. The behavior is often studied in cornstarch and water dispersions [1], and one can get a sense of the behavior at home by slowly spoon mixing roughly equal masses of these two readily available ingredients and then varying the rate of stirring.

The forms of shear thickening observed vary from a very mild version that is explainable based on the structure generated in suspensions with lubricated hard-sphere interactions [2,3], through increasingly strong thickening as the solid fraction ϕ increases until reaching a very abrupt change with increase of $\dot{\gamma}$ known as discontinuous shear thickening (DST). The range of shear thickening behaviors is illustrated using simulation data by the method of Mari and co-workers [4,5] for a non-Brownian suspension in Fig. 1; an even broader range of shear thickening in a single suspension of colloidal spheres at varying ϕ is shown in the experimental study using polymeric spheres in D'Haene *et al.* [6], with similar behavior seen for silica spheres in Cwalina and Wagner [7]. Discontinuous shear thickening implies an increase of the stress without an increase of shear rate, which can be expressed mathematically by seeking a scaling of $\eta \sim \sigma^{\beta}$ in the shear thickening region. This relation with $\beta \geqslant 1$ implies DST, since $\dot{\gamma} \sim \sigma/\eta$ is a constant for $\beta = 1$, the onset of DST. Whether strong thickening will occur depends on details of the surface interactions, as one would expect and consistent with the scenario presented here to explain the phenomena described.

*morris@ccny.cuny.edu

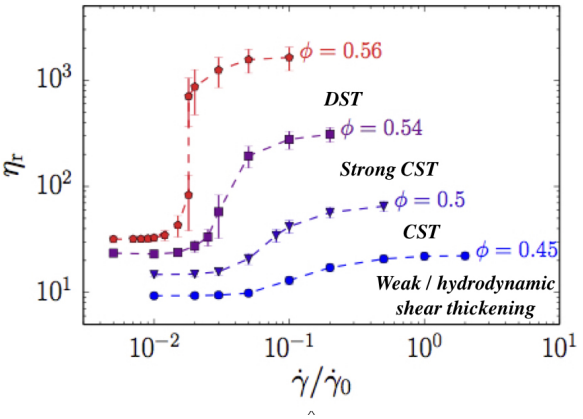

FIG. 1. Shear thickening regimes. Data from simulation by the method described by Mari *et al.* [5] illustrate weak or hydrodynamic shear thickening at volume fraction $\phi = 0.45$, continuous shear thickening at $\phi = 0.5$, strong CST at $\phi = 0.54$, and discontinuous shear thickening at $\phi = 0.56$, for a mixture of equal volume fraction non-Brownian particles of radii a and $1.4a$. The CST condition differs from the weak or hydrodynamic thickening by having dominant frictional contact stress above the thickening shear rate. The scaling of the shear rate is $\dot{\gamma}_0 = F_R/6\pi\eta_0 a^2$, where F_R is the maximum magnitude of the repulsive interparticle force (at contact) and η_0 is the fluid viscosity.

The methods used to develop results presented here have been described elsewhere, and many of the results have appeared in similar form. Thus the description of methods will have only sufficient detail to allow the reader to understand the salient features without immediate support from other work. It is hoped that with this perspective readers will be motivated to consider the references and many other studies unmentioned (simply for brevity) in order to form their own opinion and hopefully seek to contribute to understanding of shear thickening (ST) and related behaviors in dense suspensions.

The term "dense" is used to imply very concentrated suspensions, with ϕ approaching the maximum flowable fraction $\phi_{\max}$, which will here be called the jamming fraction ϕ_J, borrowing terminology arising from the granular flow community. This emphasizes the connection to the jammed solid state, a state able to statically bear shear stress in the direction of original application but failing if the load is changed in direction sufficiently. This is a key point in the physical scenario developed in this work, which involves solid contact with friction, and seeks to explain the ST occurring under conditions that are quite close, with respect to both solid fraction and stress, to a jammed state. This scenario is based on the assumption that fluid films between particles can fail to maintain separation between the surfaces and thus the interaction undergoes a lubricated-to-frictional (LF) transition, which is reflected in an increase in the apparent viscosity of the suspension.

Lubricated interactions through thin films between particles transfer momentum proportional to their relative motion, i.e., the force resisting relative velocity of a pair of particles is proportional to the velocity itself by this viscous mechanism. By contrast, solid contacts can support forces without motion and, importantly, they also support torques when the contacts are frictional. A network of solid contacts must arise to allow jamming and it is well known that friction reduces the volume fraction needed for a jammed state owing to the torques associated with frictional contacts reducing the number of contacts to achieve an isostatic condition [8]; common experience with compacting sand in a bottle by tapping to momentarily open contacts and allow settling illustrates the concept.

It is important to highlight that the underlying philosophy behind much of the work described here is that, as either the stress or solid fraction is increased, a contact network cannot form instantly from noncontacting particles at the jamming point. This implies that solid contacts are introduced at conditions well away from jamming and the volumetric density of these contacts depends on the

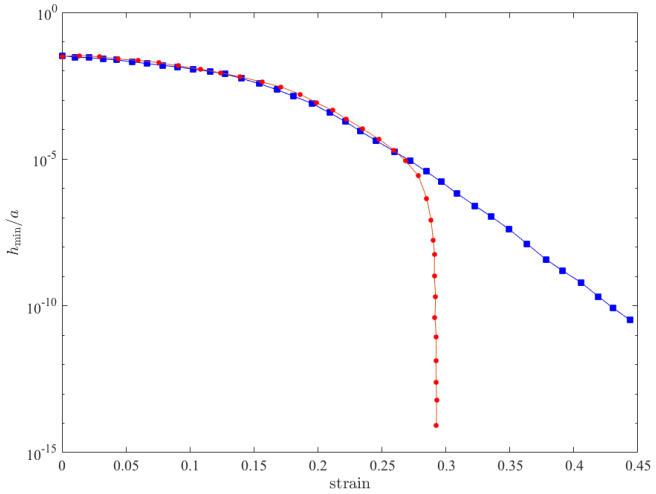

FIG. 2. Lubrication breakdown. The average minimum gap between particle surfaces normalized by the particle radius $h_{\min}/a$ is plotted as a function of the imposed strain in a simulated simple shear flow of a monodisperse hard-sphere suspension of solid volume fraction $\phi = 0.51$ in Stokes flow. These representative curves, adapted from Ref. [13], have the same time step $\dot{\gamma}\delta t = 5 \times 10^{-4}$ for predictor-corrector (red circles) and Runge-Kutta (blue squares) integration schemes, which are $O(\delta t^2)$ and $O(\delta t^4)$, respectively.

applied stress as well as the solid fraction ϕ. Simulations [4,5,9] and a mean-field theory [10] which consider a transition from lubricated-to-frictional contacts show that this basic idea, when combined with a repulsive force to "protect" against contact and thus maintain lubricated interactions at low stress, is sufficient to rationalize much of the behavior in DST and even shear jamming [11].

A conceptual difficulty with the LF transition is that, by allowing contact, it requires breakdown of the fluid mechanical description. In particular, for the case of smooth spherical particles, the fluid mechanical forces associated with lubrication are expected to maintain finite separation between surfaces. One could argue that nonsmooth shape or surface roughness will allow contact [12], but even for hard spheres, the concept of lubrication breakdown [13] supports the assumption that subcontinuum physics must play a role in the close interaction of particles in sheared suspensions. Thus we focus on the near-hard-sphere case, primarily to facilitate study by numerical simulation of a system which closely replicates a body of experiments for which the full range of ST has been seen [6,14–18]. The lubrication breakdown concept is illustrated in Fig. 2, showing that even with extremely careful simulation, a sheared suspension of rigid spheres interacting only through hydrodynamics in Stokes flow (zero Reynolds number) at $\phi = 0.5$ comes to a minimum surface separation of $O(10^{-10})$ radius in less than unit strain. For typical colloidal particles, this results in the prediction of surface separations far below atomic diameters and thus certainly implies a loss of fidelity of the continuum description of the interaction.

If contact between particles is assumed to take place, it is natural to include friction in the contact mechanics, but some uncertainty arises because the contact zone is of nanometer scale for colloidal particles. Experiments described below suggest that Coulomb friction is a reasonable description even for micron-scale spheres, although friction at this scale is certainly not a fully understood issue. In the work described here, we assume contact with friction, and this brings a qualitative change, relative to lubricated contacts, in the relation between normal and tangential motion of the solid surfaces at the closest approach or contact point. Major consequences for the bulk rheological response result from this change in the local dynamics for a highly loaded suspension.

Since the phenomena in the contact zone between micron-scale particles are on scales measured in nanometers, the details at the surface must be expected to influence behavior. At the same time,

the closeness of strong CST and DST to the jamming condition, where a system-spanning contact network is formed, demands analysis of the statistical physics on a large scale. Both the microscopic and bulk scales thus offer exciting directions for further study, and it is a challenge for the future to establish clearly how surface chemistry and surface morphology affect both the particle-scale mechanics and bulk material dynamics.

II. SELECTIVE REVIEW

Some of the earliest published work on suspension properties considered very strong shear thickening [19]. The behavior of pastes formed from cement powder and water also exhibit shear thickening alone [20] or in concrete [21] and thus practitioners working with mortars must surely have encountered conditions of ST for many centuries. From a practical perspective, strong ST is often detrimental in these applications. However, it is possible to put the phenomenon to good use, and in this direction Wagner and co-workers have made a great deal of progress in development of shear thickening fluids for body armor [22], even using specialized liquids with very low vapor pressure for astronautical space-suit application [23]; low vapor pressure is critical in case of penetration of the suit, e.g., by a micrometeorite or some accident, so that the liquid does not rapidly evaporate in the vacuum of space. The use of ST in such protective applications has recently been reviewed [24].

One of the earliest quantitative studies of shear thickening was the study of Metzner and Whitlock [25], who proposed that disturbance of smoothly gliding layers leads to a more disordered state with large-scale disturbance flows and a "dilatant" response. The term dilatant suggests that the plates driving the flow, and separated along the gradient direction of the viscometric flow, experience a thrust tending to push them apart. The term became synonymous with ST, suggesting that much of the early work on the phenomenon considered cases which showed this behavior, which is actually indicative of a positive first normal stress difference $N_1 = \sigma_{11} - \sigma_{22}$, where 1 and 2 denote the flow and velocity gradient directions in a viscometric flow, respectively (3 is the vorticity direction). As there are many examples now available from both simulation and experiment showing ST with $N_1 < 0$, it is safe to say that dilatancy and ST are separate behaviors, but under certain conditions of strong increase of the flow resistance the two are probably correlated.

A pioneering study by Hoffman [14] showed that a suspension of spheres (specifically latex particles in dioctyl phthalate) at $\phi \geqslant 0.51$ could exhibit DST with an increase of more than an order of magnitude in the viscosity. In Hoffman's work, the low-viscosity state was highly ordered, while the thickened state was disordered, with the microstructure probed by white light scattering. It was thus argued that DST was attributable to an order-disorder mechanism. Boersma *et al.* [15] and Maranzano and Wagner [17] subsequently showed that bidisperse suspensions exhibit DST, as do cornstarch dispersions, and neither show ordering, so this mechanism is not the basis for DST. However, the idea that there is a threshold stress at which the shearing forces overwhelm an interparticle repulsion, developed by Boersma *et al.* from arguments of Hoffman, resulted in a scaling analysis to rationalize the onset of ST. This work sought to explain the size dependence, as $\sigma_{\text{on}} \sim a^{-2}$, which Barnes [26] had deduced from a significant experimental database available in the literature at that time.

These scaling approaches have been further pursued [17,27,28] to provide significant insight to the factors controlling σ_{on}, the stress for onset of ST. The basic idea is to determine the upper stress limit of the low-viscosity state, by balancing a repulsive force with the shearing stress to determine at what stress particles are no longer maintained at separations that keep a lubricating layer between them. Thus, these approaches address the onset of shear thickening, but not the behavior following thickening. However, implicit in the theories is the idea that for stresses above a threshold, the classical lubrication layer becomes insufficient and a different mechanism for stress transmission must enter. Hydrodynamically interacting particles in chains aligned near the compressional axis, or hydroclusters, have been seen since the earliest Stokesian dynamics simulations [29,30] and appear to play a significant role in the onset of shear thickening by establishing the conditions for a different mechanism for momentum transfer. However, alone they are insufficient to explain

the high-viscosity state. This is seen by comparison of the viscosity predictions of suspensions of $\phi \approx 0.5$ from simulation [31] with experiment [7], shown in the latter reference. Even at extremely large concentrations $\phi = 0.585$, a Brownian hard-sphere suspension thickens only by less than a decade from its viscosity minimum and does so with a weak $\partial\eta_r/\partial\dot{\gamma}$ slope [32]. The basis for this insufficiency of hydrodynamics is that, while fluid films of thickness ϵa with $\epsilon \ll 1$ transfer momentum efficiently, and thus they contribute significantly to viscosity, they ease the motion relative to the more constrained relative motion of the contact points in a frictional interaction. In fact, these films have a tangential resistance ($\sim\ln\epsilon$) that is vanishing relative to resistance to normal motion $\sim\epsilon^{-1}$. Defining the hydrodynamic friction coefficient as the ratio of the tangential to normal resistance, $\mu_{\text{hydro}} \sim \epsilon\ln\epsilon \to 0$ as $\epsilon \to 0$: Simply stated, fluid films lubricate the flow in the colloquial as well as in the technical sense.

The concept of lubrication breakdown noted in the Introduction was described by Melrose and Ball [13], who made a detailed study of the motion of suspensions of rigid spheres in Newtonian solvent undergoing Stokes flow (Reynolds number zero), with no nonhydrodynamic interactions. They concluded that this system is pathological, as the perfectly reversible Stokes-flow motion carries a sufficiently concentrated suspension ($\phi = 0.51$ certainly qualifying) into a state of arbitrarily small surface separations: the suspension jams. Presumably the motion should retrace back to the original state if sufficiently accurately computed and then proceed to a jammed state in the reverse direction. This indeed is an apparent pathology, and a very interesting one. For present purposes, it motivates the expectation that continuum hydrodynamics must break down in the region of close approach of particle surfaces and allow a form of contact. As a consequence, repulsive forces between surfaces play a protective role and the contact interaction must be modeled to capture the dynamics for stresses above σ_{on}.

A number of studies have considered possible interactions in the contact region. Efforts focused on added dissipation within this region include those of Catherall *et al.* [33], who employed several models of surface coatings, with agreement in comparison with experimental DST found to be best for a model of a polymeric brush coating through which squeezing flow increased the dissipation [34]. While encouraging at first sight, these descriptions apply only to suspensions with fairly dense polymer brush layers, while a body of experimental work shows DST with either very-short-chain surface layers [16,17] or bare surfaces [35]. A study that showed the importance of roughness on colloidal suspension rheology by Castle *et al.* [36] went largely unnoticed. More influential work in this direction was presented by Lootens *et al.* [35], who showed that etching smooth micron-scale silica spheres, to generate root-mean-square roughness of approximately 1% of the sphere radius, resulted in a large reduction in the onset stress for shear thickening. They also reported a change in sign of N_1 from negative to positive at the thickening. In the dilatant materials ($N_1 > 0$), large normal stresses were found, with $|N_1/\sigma| > 1$. Melrose and Ball [37,38] simulated suspensions in shear and considered the network formation for various models of the contact interaction. The interactions were always frictionless, i.e., an $O(1)$ relation between the maximum tangential force and the normal force of nearly or truly touching particles was not considered, and DST was not reproduced.

We now address the LF scenario. The essential motivation for introducing the contact interactions necessary for frictional interaction is the noted inability of a rigorous hydrodynamic description to capture strong shear thickening, as seen in Stokesian dynamics results [2,31] compared with experiments [6,7]. In work from the author's group, the basic elements of lubricated contacts, repulsive forces between the particles, and allowance for contact with friction were combined in a simulation tool. This combines lubricated interactions with a discrete-element model (DEM) contact description and was named lubricated flow DEM or LF DEM; the DEM method was pioneered by Cundall and Strack [39] to describe the motion of many contacting bodies, and the approach used follows closely the original methodology. The simulations for non-Brownian particles were described by Seto and co-workers [4] (and in a more detailed form later [5]), with subsequent extension to Brownian particles [40]. Ness and Sun [41] have simulated suspension flow by a similar model, considering a wider range of conditions (showing that inertia enters but at much higher shear rates than frictional thickening), while others have utilized molecular dynamics approaches in which

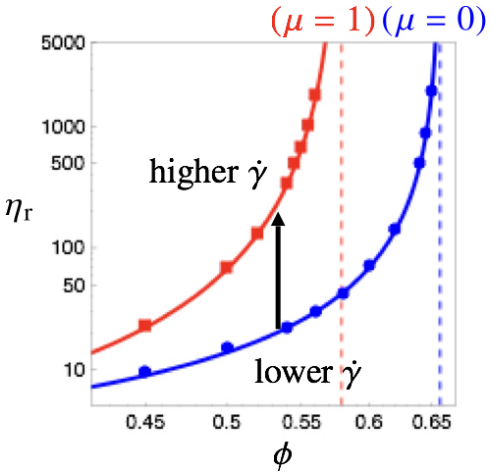

FIG. 3. Illustration of the two-state concept underlying the lubricated-to-frictional scenario. The lubricated ($\mu = 0$) and frictional ($\mu = 1$) jamming points are indicated by the labeled vertical dashed lines. At very low shear rate or stress, all close interactions are completely lubricated so that $\mu = 0$, while at very large shear rate or stress, all possible interactions which can do so have become frictional. A transition driven by shear rate of stress as indicated by the arrow takes the material to a state with a viscosity curve of lower jamming fraction and thus increases the viscosity.

the fluid and thus lubrication are not considered, but friction is activated at sufficiently large stress [42]. The latter approach showed the potential for frictional contacts to support shear jamming (SJ).

The LF scenario provides a rational basis for the rate dependence and a fairly simple model for the physical interaction leading to more efficient stress transfer in the thickened state. This two-state concept was modeled by Wyart and Cates [10], similar to earlier work by Bashkirtseva *et al.* [43], in which the fraction of frictional contacts is modeled as a function of the particle pressure [44] Π, i.e., as $f(\Pi)$. The shear stress is more readily controlled both experimentally and in simulation studies, and Π increases when σ increases, so $f(\sigma)$ provides a more accessible description of this quantity. From sampling of simulations [5], $f(\sigma) = \exp(\sigma^*/\sigma)$ is determined, with $\sigma^* \approx 1.45 F_R/a^2$. As described in more detail in Sec. IV, this captures the two-state concept through the key idea that as f increases, the jamming packing fraction becomes a function of the applied stress $\phi_J(\sigma)$ and varies smoothly from a maximum at the frictionless value ϕ_J^0 at $\sigma \ll F_R/a^2$ to the smaller frictional value $\phi_J(\mu)$ or in shorthand ϕ_J^μ. The rheological functions then have dependences on solid fraction which, based on comparison against simulations, are well captured by the functional forms $\eta \sim [\phi - \phi_J(\sigma)]^{-2}$, with the second normal stress difference and Π both scaling as $\phi^2(\phi - \phi_J(\sigma))^{-2}$ [9]. The first normal stress difference changes sign, and apparently depends more critically on detailed microstructure (e.g., perhaps on the near contact pair distribution function), and thus the quality of this model for N_1 is less satisfactory; the change of sign and the relevance to assessment of lubricated and frictional rheologies of suspensions have been examined [45] but are not fully resolved. The essential physical concept to bear in mind in this model is illustrated by Fig. 3, which shows that as stress (or shear rate) increases, the suspension behavior transitions from a lower-viscosity curve to a higher one, with the difference resulting from this reduction in the jamming fraction owing to activation of frictional contacts. The behavior depends on ϕ, with more rapid increase of the stress with imposed shear rate as ϕ increases. Note that if the volume fraction is above the jamming fraction for frictional interactions, i.e., $\phi > \phi_J^\mu$, then the thickening carries the viscosity to infinite values, implying shear jamming.

The details of particle contact depend on the environment at the particle surfaces and in the narrow gap formed as two surfaces become very close, and thus in principle many factors may come

into play, including the hardness of the solid and its potential deformation and whether the surfaces bear charge or are coated with surfactant or polymer. Hence, the LF transition approach and the contact model described in the prior paragraph cannot describe all states without added parameters, and it is too simple to expect it is a complete representation of any specific case. However, the scenario appears to capture the salient features of strong CST, DST, and SJ, including the recent finding from experiments that contact stresses can be the dominant rheological contribution in a dense suspension. Lin *et al.* [46] showed that the shear stress drops from its steady value σ_{ss} to σ_{rev} when the shearing direction is suddenly reversed, and then grows back to the original steady value over a strain of $O(1)$. The hydrodynamic shear stress, which has the same value upon reversal, is σ_{rev} and the difference $\sigma_{ss} - \sigma_{rev}$ is the stress resulting from nonhydrodynamic forces. Lin *et al.* complemented their experiments with simulations using the method of Mari *et al.* [5] to deduce for near-hard-sphere suspensions that this difference was consistent with development of contact stress.

Direct measurements of the contact friction between particles have recently been reported. As an example, Comtet *et al.* measured the friction of 1-μm-diam particles of poly-vinyl chloride against a plane surface of the same material, with the surfaces immersed in a plasticizer, and correlated the frictional behavior with the shear thickening response of the bulk suspension of the same components [47]. These authors reported average friction coefficients of $\mu \approx 0.5$ and reported rheological behavior in qualitative agreement with the LF scenario. Fernandez *et al.* used atomic force microscopy measurement to study the friction between 10-μm silica spheres, finding that μ varied from 0.05 for surfaces covered by polymer brushes to 0.9 for "clean" particles (no polymer or contaminants on their surfaces) [48]. As noted above, particle roughness affects suspension rheology. While there is expected to be a relation between roughness and friction, roughness introduces a length scale (typically small relative to the particle radius, but surely finite) which the friction description does not. The role of this length scale, and its relation to the measured friction, is of interest, and recent efforts to probe this issue through creative methods of synthesizing roughness [49,50] offer an alternative to generating roughness by etching particle surfaces [35].

III. ELEMENTS OF SHEAR THICKENING

From the foregoing it may be deduced that there are three basic elements needed to describe the shear thickening in the lubricated-to-frictional scenario [4], and the influence of the frictional effects becomes dominant in the thickened state only for solid fractions greater than $\phi \approx 0.5$. The first is that the particles interact hydrodynamically, so surface motions of close pairs are strongly influenced by lubrication stresses. While lubrication can generate large forces, tangential motion of the positions of closest approach mediated by a lubrication film at a given normal force is substantially less restricted than a frictional solid contact.

The second element is a repulsive interaction, which maintains surface separation and lubricated contacts up to a characteristic stress. The repulsive force may arise from electrostatic double layer overlap, or polymer brush interactions, for example. The role of the repulsive interaction is central to the shear rate dependence of the material properties seen in DST. It is against this repulsive force that the shearing force bringing a pair of particles together must be balanced to transition from the lubricated-to-frictional regime of particle interaction. This characteristic shear force may be written as σa^2, with the particle size a taken as the radius for spheres. When balanced against F_R, a characteristic stress based on the microscopic interaction may be defined as $\sigma_0 = F_R/6\pi a^2$, and we define a dimensionless stress $\tilde{\sigma} = \sigma/\sigma_0$. The characteristic shear rate defined similarly is $\dot{\gamma}_0 = \sigma_0/\eta_0$.

The final element is that contact must occur. However, it is important that the contact be frictional: A simple normal contact model with tangential slip resisted only by hydrodynamics and not by a solid contact mechanism does not cause a significant increase in the flow resistance. The contact force introduces solid mechanical properties, and in our simulations, these are softer than realistic particles in ST suspensions; Townsend and Wilson [51] have noted the importance of the softness, which may be associated with the need for enduring contacts in order to obtain strong ST.

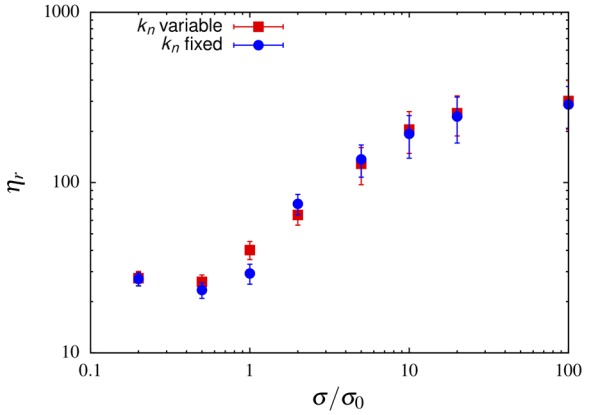

FIG. 4. Viscosity from simulation at $\phi = 0.54$ for two protocols, one using a constant spring stiffness, at the value determined to maintain a maximum linear deformation of $0.03a$, with a the particle radius, at the highest stress, and the other using a variable stiffness sufficient to maintain a maximum deformation of $0.03a$ at each condition (hence a lower stiffness at lower stress). The stress scaling is $\sigma_0 = F_R/6\pi a^2$, where F_R is the maximum repulsive force magnitude at contact.

The presence of finite stiffness necessitates a choice of how one simulates the behavior. The elastic normal force is given by $F_{\text{el}} = -k_n\delta_n$, where k_n is the spring stiffness and δ_n is the deformation of the surface. If the particle stiffness is fixed, then at different stress levels, the deformation varies such that the geometry of the suspension changes: Unless volume is explicitly tracked (it is not in our own simulations to date [4,5,52]), then the effective volume fraction can change. This is a satisfactory model if the stiffness found to agree with a maximal deformation of particle surfaces at large stress is applied at all lower stresses as well so that there is a very limited effect of volume loss. This has no effect at small stress where contacts are infrequent, but proves to be computationally expensive in the transition regime, as the time step must be reduced to quite small values to capture the weakly deformed contact interaction faithfully (allowing it to be enduring and not an erratically computed interaction). The alternative is to consider a variable stiffness spring which allows a similar deformation at each stress level. Provided this deformation level is small (typically 2–3% of the particle radius is the maximum allowed in our work), this gives behavior consistent with experimental observation [5]. In Fig. 4, the results of these two approaches for maximum linear deformation of $\delta_n/a < 0.03$ are shown to be essentially the same for a friction coefficient of $\mu = 1.0$ at $\phi = 0.54$. This friction coefficient is somewhat larger than the values found in experiments noted above [47].

IV. RESULTS FROM THE LF SCENARIO

We present here a brief sequence of results summarizing primary predictions of the LF scenario. In shear thickening suspensions, the viscosity increase becomes increasingly large, and the rate of increase also rises, with an increase in ϕ. This was clearly shown in the work of D'Haene *et al.* [6], who considered polymeric [poly(methyl methacrylate)] particles in a Newtonian solvent for $0.276 \leqslant \phi \leqslant 0.641$; essentially rate-independent viscosity was found at the lowest fractions, giving way to weak or hydrodynamic thickening for $\phi \approx 0.35$–0.45, increasingly strong CST as ϕ increased up to $\phi = 0.557$, and DST for $\phi = 0.575$. As shown in Fig. 1, simulation results by the method noted above [5], spanning the shear thickening range for a friction coefficient of $\mu = 1$, show the same behaviors: weak thickening at $\phi = 0.45$, CST going from $\phi = 0.46$ to 0.54, and DST for $\phi = 0.56$. For $\phi > 0.59$, D'Haene *et al.* observed that an increase of stress resulted in a decrease in shear rate, suggestive of shear-driven jamming, and this behavior has more recently been elucidated for cornstarch dispersions by Peters *et al.* [11]. We return to SJ below.

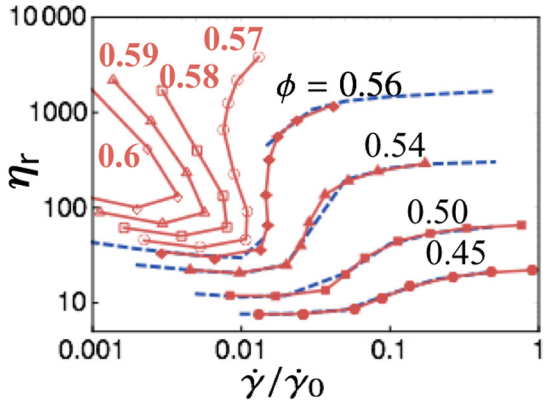

FIG. 5. Results from shear rate- (blue dashed lines) and shear stress-controlled (symbols and red solid lines) simulations [52], showing equivalence of results up to onset of DST, with shear rate control allowing exploration of the S-shaped curves associated with DST, as well as shear jamming.

By using shear stress control, it is found in simulation [52] and experiment [53] that rather than a discontinuity in viscosity, one may access an S-shaped curve describing the stress or viscosity when plotted as a function of shear rate; under rate control, the multivalued part of the curve is not accessed. The equivalence of results obtained with controlled shear rate or shear stress up to the viscosity discontinuity at $\phi = 0.56$ is shown in Fig. 5, which also shows the S-shaped curves associated with DST having larger jumps in the viscosity for $\phi = 0.57$–0.59 and SJ for $\phi \geqslant 0.6$. The SJ is characterized by $\eta(\dot{\gamma})$ curves which access only the lower range of shear rates: In these stress-controlled simulations, as the stress increases the viscosity curves turn toward progressively smaller shear rates until the material stops flowing. While one may expect instability to shear banding in the S-shaped region of the flow curves, the methodology applied determines a single shear rate for the periodically replicated simulation cell and forces single-domain behavior. A more faithful representation of experiments, in which walls drive the flow, might show different behavior. Hermes *et al.* have argued based on the inability to simultaneously balance shear and normal stresses at the boundary between two shear bands that steady shear banding is not expected in dense suspensions [54].

For the friction coefficient $\mu = 1$ yielding the results of Figs. 1 and 5, $\phi_J^\mu \approx 0.59$, and simulations for $\phi > \phi_J^\mu$ show the noted shear jamming. This can be understood based on the model of Wyart and Cates [10], which captures the shear thickening transition by introducing a mixing rule for the jamming fraction:

$$\phi_J(\tilde{\sigma}) = f(\tilde{\sigma})\phi_J^\mu + [1 - f(\tilde{\sigma})]\phi_J^0, \tag{1}$$

where it is recalled that $f(\tilde{\sigma})$ is the fraction of close interactions which are frictional and $\tilde{\sigma} = \sigma/\sigma_0$. Then the viscosity can be written using a viscosity function of the Krieger [55] form but with stress dependence embedded in the jamming fraction, $\eta_r(\phi, \tilde{\sigma}) \sim [\phi - \phi_J(\tilde{\sigma})]^{-2}$. The results of this model are illustrated in comparison with a large database of simulation results spanning the CST, DST, and SJ regions in Fig. 6(a). These results are consolidated into a flow-state (or phase) diagram showing the regions in the ϕ-$\tilde{\sigma}$ space shown in Fig. 6(b), for the particular case of $\mu = 1$ from Singh *et al.* [9]. The role of increasing friction coefficient, which decreases the jamming fraction, is shown in Fig. 6(c) for different μ based on the constitutive model derived from the theory of Wyart and Cates and informed by the simulations of Singh *et al.* Larger friction coefficient μ results in an expanded region of both DST and DST-SJ. The structure of the phase diagram is quite similar to that developed based on experimental results for a cornstarch dispersion [11].

The results presented above are all for non-Brownian suspensions, and for simplicity we do not consider Brownian suspensions in detail. However, most of the experimental studies delineating

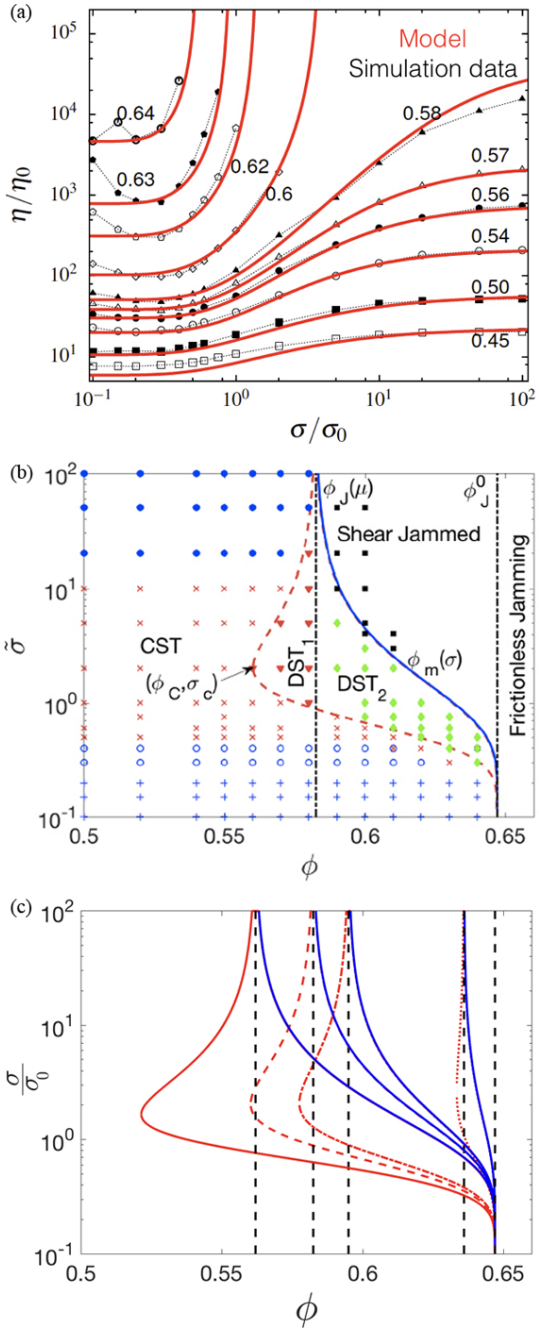

FIG. 6. Flow states. (a) Constitutive model [9] compared with simulation for $\mu = 1$ with equal parts of particles of relative size 1 and 1.4. (b) Flow state diagram for conditions of (a). The dashed vertical lines indicate the frictional jamming fraction of $\phi_J^\mu \approx 0.585$ and the frictionless jamming $\phi_J^0 \approx 0.65$. DST_1 (inverted triangles) indicates a transition between two flowing states and DST_2 (diamonds) implies thickening to a shear-jammed state (squares); regions of shear thinning (+) and rate-independent viscosity (open and closed circles at low and high stress, respectively) are indicated. (c) Combined flow state diagram boundaries for different friction coefficients, with jamming fractions illustrated by the dashed vertical lines: The rightmost is ϕ_J^0 while the others are ϕ_J^μ decreasing through the sequence of $\mu = 0.1$, 0.5, 1, and 10.

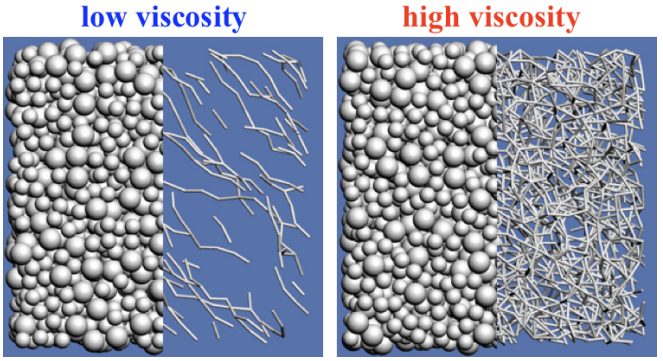

FIG. 7. Particle configurations and frictional contact force network for $\phi = 0.54$ and $\mu = 1$ (strong CST) in the low-stress low-viscosity (high-stress high-viscosity) state on the left (right); the low-viscosity state is in the initial weak increase of the viscosity curve [$\sigma/\sigma_0 \approx 0.5$ in Fig. 6(a)]. Shear flow velocity increases from the bottom to the top of the image, indicating the orientation of force chains near the compressional axis in the low-viscosity state.

ST in suspensions of spherical particles have considered submicron particles [6,16,17,56] and thus inclusion of Brownian motion is an important consideration. Brownian motion acts as a spring force which tends to keep particles separated, and our recent work found that results of Cwalina and Wagner [7] for both η_r and the second normal stress difference $N_2 = \sigma_{22} - \sigma_{33}$ could be matched well by including a repulsive force along with Brownian motion. However, these simulations notably fail to match $N_1 = \sigma_{11} - \sigma_{22}$ from the same experiments, and this suggests that the microstructure related to the first normal stress difference depends on details of the close interaction which are not needed to obtain good agreement with η_r and N_2 [7].

The microstructural change that takes place at the LF transition is not readily found in the positional correlation. As shown by Mari *et al.* [5], the structural changes seen in the pair correlation function are subtle. On the other hand, the frictional force network displays striking changes across the LF transition. In the portion of the flow curve showing the onset of ST, extended and fairly linear chains of particles (which in fact grow from hydroclusters) interacting through frictional forces, aligned near the compression direction, are observed. These structures grow with increasing stress. At the thickening transition for sufficiently large ϕ, the chains percolate in all directions to form a more isotropic and dense network. The percolation of the frictional force chains gives a giant connected component in terms of graph theory, as considered in Ref. [57]. Images from the low-viscosity and high-viscosity states showing this behavior were developed from simulations of the LF transition [4,5], and a similar set of images for a strong CST suspension of $\phi = 0.54$ and $\mu = 1$ is shown in Fig. 7.

V. PERSPECTIVE

The goal of this article is to provide insight into a recently proposed scenario that captures elements of shear thickening in dense suspensions. As a practical definition, $\phi = 0.5$ serves roughly as a boundary between semidense and dense conditions [57] in monodisperse (or nearly so) suspensions. For $0.35 < \phi < 0.5$, the suspension viscosity is well above that of the suspending fluid and the normal stresses and associated particle migration effects [58] are significant, while ST occurs but is hydrodynamically controlled and weak. For Brownian particles, a purely hydrodynamic description of the mechanics has been shown to capture this behavior [2,31]. For $\phi > 0.5$, the ST intensifies and a nonhydrodynamic mechanism is needed to rationalize the stresses generated. The lubricated-to-frictional scenario in which lubricated interactions between particles give way to frictional contacts at an onset stress determined by a repulsive (protective)

colloidal force provides a description capturing many of the experimentally observed phenomena. This scenario has been considered in both simulation [4,5,40,52] and theory [10,43] and recently developed in a constitutive description [9].

Strong ST or SJ are often problematic in applications. As noted, these behaviors reduce workability of cement-based materials, while they can disrupt coating [59] or extrusion processes. In the latter case, closeness to jamming has been related to self-filtration in which the solid concentration in the reservoir drops as it passes the constriction into the die [60]. This phenomenon is associated with an instability to a periodically varying extrusion rate of dense suspensions [61,62]; a conjecture is that the instability is related to the time-dependent flow appearing in shear flow under DST conditions [54]. In light of the recent work on shear thickening, it is thus valuable to consider possible mitigation and control of the behaviors on one hand or ways to exploit the ST phenomenon on the other. Coatings which maintain surface separation and allow ready tangential motion of particle surfaces are a straightforward approach to mitigation, and these can be more readily designed if the mechanistic basis is better understood. In a quite distinct approach, shearing protocols which mix a primary unidirectional shear with an orthogonal oscillatory shearing have been studied and shown to reduce the apparent viscosity drastically over a particular range of the oscillatory component [63]. This tunable nature of shear thickening apparently arises from controlled disruption of the force network. The application of an orthogonal oscillation thus provides a means of effecting major change in flow properties without changing composition, an approach that is especially interesting if the ultimate use of the flowing material does not allow additives. Studies which consider these flow protocols, as well as general flow modeling, for dense suspensions could thus provide both insight into the material behavior and very useful engineering tools.

In considering the present state of investigation of ST, it is useful to establish what appears to be clearly understood about ST in dense suspensions and what issues remain unclear. Based on a number of factors, classic lubrication between particles is clearly insufficient, both to maintain surfaces separated to allow smooth tangential relative motion and to explain the added viscosity above the transition to a thickened state. The description of lubrication breakdown [13] shows mathematically that, even for smooth surfaces, the separation vanishes for sufficiently large ϕ, implying a failure of the continuum fluid mechanical description of the phenomena in the film between particles, while surface roughness or sharp edges allow contact in finite time in the classic fluid mechanical description [12]. Thus, acceptance of a contact of a form similar to that occurring in dry granular flows seems to be fully warranted; yet in order to establish fundamental understanding of dense suspension rheology, particularly the strong versions of ST, examination of the basis for lubrication breakdown would be useful. An added point that is clear is that some nonhydrodynamic force must balance the shear-driven forces to yield rate dependence, with colloidal forces of electrical origin one possibility. The magnitude of this repulsive force sets the characteristic stress for the onset of ST. Deformation of particles could play a role, but this would be expected to occur only at higher stresses, thus limiting the magnitude of the stress increase [64]. We can safely say that the near-contact interactions between particles play a predominant role and that the more extreme versions of ST are not explained by hydrodynamics between smooth surfaces. Thus, ST and other dense suspension rheological behaviors are influenced by interparticle tribology.

The tribology of colloidal particle surface interactions has only recently attracted significant study. Methods of force microscopy have been applied to measure friction [47] and roughness [35,50], but there remains a wide range of questions. These are likely to require consideration of molecular-scale processes, since contact localizes forces to nanometer-scale regions on particle surfaces. The resulting local stresses are very intense and thus it may not only be the lubrication properties between surfaces that play a role: Surface coating damage or plastic deformation and wear of coatings, or particles themselves, seem to be topics of relevance.

An issue that certainly warrants consideration is the fact that strong CST and DST occur for quite a range of particle-liquid combinations [26,65], for each of which the forces at microscale will be different. The similarity of the properties at macroscopic scale for various suspensions is suggestive of a pseudocontinuum interaction at the surfaces and may be the basis for success of

the relatively simple friction model used in exploring the LF scenario to date. It is well known in colloidal rheology that surface coatings may play a major role, for example, serving as an aid to workability of cement and concrete. There is a potential for improvement of methods of surface modification by coupling molecular understanding to the mechanical analyses which form the focus in this article. In this direction, a recent study [66] introduces the possibility that hydrogen bonding in the gap between particles plays a role. Finally, it was noted that repulsive forces enter in a scaling for the onset stress $\sigma_{on} \propto F_R a^{-2}$. Since it is expected that the repulsive force will itself have an a dependence, with this dependence different for Brownian, electrostatic, and steric stabilizing forces [17], the observation of size scaling of $\sigma_{on} \sim a^{-2}$ is unclear [56].

One point that is quite surprising is the apparent reversibility of DST in colloidal suspensions. It is commonly expected that colloidal particles in contact experience strong van der Waals attractions. For particles carefully tailored to be refractive index matched to the solvent, the van der Waals forces can be minimized [67], but for the general case, cohesion is expected. The influence of strong attractive or cohesive forces between particles has been considered and shown to lead to large low-shear viscosity or a yield stress, thus reducing the extent of, or totally obscuring, ST [68–70]. There has been little examination of how weaker attractions might affect the fine details of structure.

Finally, we consider the interaction of scales. The issues noted above for further study are at particle or contact scale. In any mechanism that transforms the ability to efficiently transmit momentum through a suspension of spheres, larger-scale structures must form. In the LF scenario, the structures are connected clusters of particles linked by frictional contacts. As illustrated by Fig. 7 for a strong CST condition of $\phi = 0.54$, these form chains that are primarily aligned along the compressional axis of the flow at stresses that approach the ST onset level, at which point these chains rapidly (as a function of stress) branch and join to form a dense network in all directions. In DST, the network growth is more abrupt as a function of shear rate and the thickened state is denser in connections. The statistical physics of this transition warrants examination. This topic is impacted by the particle scale forces, but demands system level considerations. Thus the lubricated-to-frictional scenario for shear thickening raises significant questions which span from nanometer-scale contacts to the macroscopic flow scale.

ACKNOWLEDGMENTS

This work was supported by NSF CBET (Award No. 1605283). The development of the perspective described in this work was made possible through collaborations with Professor M. Denn, Dr. R. Mari, Dr. R. Seto, Dr. A. Singh, S. Pednekar, and O. Sedes (all presently or formerly at CUNY City College of New York) and has benefited from discussions with Professor B. Chakraborty (Brandeis University).

[1] A. Fall, A. Lemaître, F. Bertrand, D. Bonn, and G. Ovarlez, Shear Thickening and Migration in Granular Suspensions, Phys. Rev. Lett. **105**, 268303 (2010).

[2] T. N. Phung, J. F. Brady, and G. Bossis, Stokesian dynamics simulation of Brownian suspensions, J. Fluid Mech. **313**, 181 (1996).

[3] J. F. Brady and J. F. Morris, Microstructure of strongly sheared suspensions and its impact on rheology and diffusion, J. Fluid Mech. **348**, 103 (1997).

[4] R. Seto, R. Mari, J. F. Morris, and M. M. Denn, Discontinuous Shear Thickening of Frictional Hard-Sphere Suspensions, Phys. Rev. Lett. **111**, 218301 (2013).

[5] R. Mari, R. Seto, J. F. Morris, and M. M. Denn, Shear thickening, frictionless and frictional rheologies in non-Brownian suspensions, J. Rheol. **58**, 1693 (2014).

[6] P. D'Haene, J. Mewis, and G. G. Fuller, Scattering dichroism measurements of flow-induced structure of a shear thickening suspension, J. Colloid Interface Sci. **156**, 350 (1993).

[7] C. D. Cwalina and N. J. Wagner, Material properties of the shear-thickened state in concentrated near hard-sphere colloidal dispersions, J. Rheol. **58**, 949 (2014).
[8] A. J. Liu and S. R. Nagel, The jamming transition and the marginally jammed solid, Annu. Rev. Condens. Matter Phys. **1**, 347 (2010).
[9] A. Singh, R. Mari, M. M. Denn, and J. F. Morris, A constitutive model for simple shear of dense frictional suspensions, J. Rheol. **62**, 457 (2018).
[10] M. Wyart and M. E. Cates, Discontinuous Shear Thickening Without Inertia in Dense Non-Brownian Suspensions, Phys. Rev. Lett. **112**, 098302 (2014).
[11] I. R. Peters, S. Majumdar, and H. M. Jaeger, Direct observation of dynamic shear jamming in dense suspensions, Nature (London) **532**, 214 (2016).
[12] P. Pakdel and S. Kim, Mobility and stresslet functions of particles with rough surfaces in viscous fluids: A numerical study, J. Rheol. **35**, 797 (1991).
[13] J. R. Melrose and R. C. Ball, The pathological behavior of sheared hard spheres with hydrodynamic interactions, Europhys. Lett. **32**, 535 (1995).
[14] R. L. Hoffman, Discontinuous and dilatant viscosity behavior in concentrated suspensions. I. Observation of a flow instability, Trans. Soc. Rheol. **16**, 155 (1972).
[15] W. H. Boersma, P. J. M. Baets, J. Laven, and H. N. Stein, Time-dependent behavior and wall slip in concentrated shear thickening dispersions, J. Rheol. **35**, 1093 (1991).
[16] J. Bender and N. J. Wagner, Reversible shear thickening in monodisperse and bidisperse colloidal dispersions, J. Rheol. **40**, 899 (1996).
[17] B. J. Maranzano and N. J. Wagner, The effects of particle size on reversible shear thickening of concentrated colloidal dispersions, J. Chem. Phys. **114**, 10514 (2001).
[18] E. Brown and H. M. Jaeger, The role of dilation and confining stresses in shear thickening of dense suspensions, J. Rheol. **56**, 875 (2012).
[19] H. Freundlich and H. L. Roder, Dilatancy and its relation to thixotropy, Trans. Faraday Soc. **34**, 308 (1938).
[20] F. Toussaint, C. Roy, and P.-H. Jézéquel, Reducing shear thickening of cement-based suspensions, Rheol. Acta **48**, 883 (2009).
[21] D. Feys, R. Verhoeven, and G. De Schutter, Why is fresh self-compacting concrete shear thickening? Cement Concrete Res. **39**, 510 (2009).
[22] Y. S. Lee, E. D. Wetzel, and N. J. Wagner, The ballistic impact characteristics of Kevlar® woven fabrics impregnated with a colloidal shear thickening fluid, J. Mater. Sci. **38**, 2825 (2003).
[23] R. Dombrowski, N. J. Wagner, M. Katzarova, and B. Peters, Development of advanced environmental protection garments containing shear thickening fluid enhanced textiles (STF-Armor^{TM}) for puncture protection and dust mitigation, *Proceedings of the 48th International Conference on Environmental Systems, Albuquerque* (STF Technologies LLC, 2018).
[24] S. Gürgen, M. C. Kuşhan, and W. Li, Shear thickening fluids in protective applications: A review, Prog. Polym. Sci. **75**, 48 (2017).
[25] A. B. Metzner and M. Whitlock, Flow behavior of concentrated (dilatant) suspensions, Trans. Soc. Rheol. **2**, 239 (1958).
[26] H. A. Barnes, Shear-thickening ("dilatancy") in suspensions of nonaggregating solid particles dispersed in Newtonian liquids, J. Rheol. **33**, 329 (1989).
[27] J. Kaldasch, B. Senge, and J. Laven, Shear thickening in electrically-stabilized colloidal suspensions, Rheol. Acta **47**, 319 (2008).
[28] J. Kaldasch and B. Senge, Shear thickening in polymer stabilized colloidal suspensions, Colloid Polymer Sci. **287**, 1481 (2009).
[29] J. F. Brady and G. Bossis, The rheology of concentrated suspensions of spheres in simple shear flow by numerical simulation, J. Fluid Mech. **155**, 105 (1985).
[30] J. F. Brady and G. Bossis, Stokesian dynamics, Annu. Rev. Fluid Mech. **20**, 111 (1988).
[31] D. R. Foss and J. F. Brady, Structure, diffusion and rheology of Brownian suspensions by Stokesian dynamics simulation, J. Fluid Mech. **407**, 167 (2000).

[32] J. F. Morris and B. Katyal, Microstructure from simulated Brownian suspension flows at large shear rate, Phys. Fluids **14**, 1920 (2002).
[33] A. A. Catherall, J. R. Melrose, and R. C. Ball, Shear thickening and order–disorder effects in concentrated colloids at high shear rates, J. Rheol. **44**, 1 (2000).
[34] A. A. Potanin and W. B. Russel, Hydrodynamic interaction of particles with grafted polymer brushes and applications to rheology of colloidal dispersions, Phys. Rev. E **52**, 730 (1995).
[35] D. Lootens, H. van Damme, Y. Hémar, and P. Hébraud, Dilatant Flow of Concentrated Suspensions of Rough Particles, Phys. Rev. Lett. **95**, 268302 (2005).
[36] J. Castle, A. Farid, and L. V. Woodcock, The effect of surface friction on the rheology of hard-sphere colloids, Prog. Colloid Polym. Sci. **100**, 259 (1996).
[37] J. R. Melrose and R. C. Ball, Continuous shear thickening transitions in model concentrated colloids–the role of interparticle forces, J. Rheol. **48**, 937 (2004).
[38] J. R. Melrose and R. C. Ball, "Contact networks" in continuously shear thickening colloids, J. Rheol. **48**, 961 (2004).
[39] P. A. Cundall and O. D. L. Strack, A discrete numerical model for granular assemblies, Geotechnique **29**, 47 (1979).
[40] R. Mari, R. Seto, J. F. Morris, and M. M. Denn, Discontinuous shear thickening in Brownian suspensions by dynamic simulation, Proc. Natl. Acad. Sci. USA **112**, 15326 (2015).
[41] C. Ness and J. Sun, Flow regime transitions in dense non-Brownian suspensions: Rheology, microstructural characterization, and constitutive modeling, Phys. Rev. E **91**, 012201 (2015).
[42] M. Grob, C. Heussinger, and A. Zippelius, Jamming of frictional particles: A nonequilibrium first-order phase transition, Phys. Rev. E **89**, 050201 (2014).
[43] I. A. Bashkirtseva, A. Y. Zubarev, L. Y. Iskakova, and L. B. Ryashko, On rheophysics of high-concentrated suspensions, Colloid J. **71**, 446 (2009).
[44] A. Deboeuf, G. Gauthier, J. Martin, Y. Yurkovetsky, and J. F. Morris, Particle Pressure in a Sheared Suspension: A Bridge from Osmosis to Granular Dilatancy, Phys. Rev. Lett. **102**, 108301 (2009).
[45] J. R. Royer, D. L. Blair, and S. D. Hudson, Rheological Signature of Frictional Interactions in Shear Thickening Suspensions, Phys. Rev. Lett. **116**, 188301 (2016).
[46] N. Y. C. Lin, B. M. Guy, M. Hermes, C. Ness, J. Sun, W. C. K. Poon, and I. Cohen, Hydrodynamic and Contact Contributions to Continuous Shear Thickening in Colloidal Suspensions, Phys. Rev. Lett. **115**, 228304 (2015).
[47] J. Comtet, G. Chatté, A. Niguès, L. Bocquet, A. Siria, and A. Colin, Pairwise frictional profile between particles determines discontinuous shear thickening transition in non-colloidal suspensions, Nat. Commun. **8**, 15633 (2017).
[48] N. Fernandez, J. Cayer-Barrioz, L. Isa, and N. D. Spencer, Direct, robust technique for the measurement of friction between microspheres, Langmuir **31**, 8809 (2015).
[49] L. C. Hsiao, S. Jamali, E. Glynos, P. F. Green, R. G. Larson, and M. J. Solomon, Rheological State Diagrams for Rough Colloids in Shear Flow, Phys. Rev. Lett. **119**, 158001 (2017).
[50] C.-P. Hsu, S. N. Ramakrishna, M. Zanini, N. D. Spencer, and L. Isa, Roughness-dependent tribology effects on discontinuous shear thickening, Proc. Natl. Acad. Sci. USA **115**, 5117 (2018).
[51] A. K. Townsend and H. J. Wilson, Frictional shear thickening in suspensions: The effect of rigid asperities, Phys. Fluids **29**, 121607 (2017).
[52] R. Mari, R. Seto, J. F. Morris, and M. M. Denn, Nonmonotonic flow curves of shear thickening suspensions, Phys. Rev. E **91**, 052302 (2015).
[53] Z. Pan, H. de Cagny, B. Weber, and D. Bonn, S-shaped flow curves of shear thickening suspensions: Direct observation of frictional rheology, Phys. Rev. E **92**, 032202 (2015).
[54] M. Hermes, B. M. Guy, W. C. K. Poon, G. Poy, M. E. Cates, and M. Wyart, Unsteady flow and particle migration in dense, non-Brownian suspensions, J. Rheol. **60**, 905 (2016).
[55] I. M. Krieger, Rheology of monodisperse latices, Adv. Colloid Interface Sci. **3**, 111 (1972).
[56] B. M. Guy, M. Hermes, and W. C. K. Poon, Towards a Unified Description of the Rheology of Hard-Particle Suspensions, Phys. Rev. Lett. **115**, 088304 (2015).

[57] A. Boromand, S. Jamali, B. Grove, and J. M. Maia, A generalized frictional and hydrodynamic model of the dynamics and structure of dense colloidal suspensions, J. Rheol. **62**, 905 (2018).
[58] J. F. Morris and F. Boulay, Curvilinear flows of noncolloidal suspensions: The role of normal stresses, J. Rheol. **43**, 1213 (1999).
[59] S. Khandavalli and J. P. Rothstein, The effect of shear-thickening on the stability of slot-die coating, AIChE J. **62**, 4536 (2016).
[60] M. D. Haw, Jamming, Two-Fluid Behavior, and "Self-Filtration" in Concentrated Particulate Suspensions, Phys. Rev. Lett. **92**, 185506 (2004).
[61] P. Yaras, D. M. Kalyon, and U. Yilmazer, Flow instabilities in capillary flow of concentrated suspensions, Rheol. Acta **33**, 48 (1994).
[62] S. D. Kulkarni, B. Metzger, and J. F. Morris, Particle-pressure-induced self-filtration in concentrated suspensions, Phys. Rev. E **82**, 010402 (2010).
[63] N. Y. C. Lin, C. Ness, M. E. Cates, J. Sun, and I. Cohen, Tunable shear thickening in suspensions, Proc. Natl. Acad. Sci. USA **113**, 10774 (2016).
[64] D. P. Kalman, B. A. Rosen, and N. J. Wagner, in *Proceedings of the XV International Congress on Rheology: The Society of Rheology 80th Annual Meeting*, edited by A. Co, G. L. Leal, R. H. Colby, and A. Jeffrey, AIP Conf. Proc. No. 1027 (AIP, Melville, 2008), pp. 1408–1410.
[65] E. Brown and H. M. Jaeger, Shear thickening in concentrated suspensions: Phenomenology, mechanisms and relations to jamming, Rep. Prog. Phys. **77**, 046602 (2014).
[66] N. M. James, E. Han, R. A. L. de la Cruz, J. Jureller, and H. M. Jaeger, Interparticle hydrogen bonding can elicit shear jamming in dense suspensions, Nat. Mater. **17**, 965 (2018).
[67] W. B. Russel, D. A. Saville, and W. R. Schowalter, *Colloidal Dispersions* (Cambridge University Press, Cambridge, 1992).
[68] V. Gopalakrishnan and C. F. Zukoski, Effect of attractions on shear thickening in dense suspensions, J. Rheol. **48**, 1321 (2004).
[69] E. Brown, N. A. Forman, C. S. Orellana, Z. Hanjun, B. W. Maynor, D. E. Betts, J. M. DeSimone, and H. M. Jaeger, Generality of shear thickening in dense suspensions, Nat. Mater. **9**, 220 (2010).
[70] S. Pednekar, J. Chun, and J. F. Morris, Simulation of shear thickening in attractive colloidal suspensions, Soft Matter **13**, 1773 (2017).